https://doi.org/10.5194/egusphere-2022-616
Preprint. Discussion started: 29 August 2022

Reconstructing five decades of sediment export from two glaciated high-alpine catchments in Tyrol, Austria, using nonparametric regression

Lena Katharina Schmidt[1], Till Francke[1], Peter Martin Grosse[1], Christoph Mayer[2], Axel Bronstert[1]

[1]Institute of Environmental Sciences and Geography, University of Potsdam, Potsdam, 14476, Germany
[2]Bavarian Academy of Sciences and Humanities, Munich, 80539, Germany

Correspondence to: Lena Katharina Schmidt (leschmid@uni-potsdam.de)

https://doi.org/10.5194/egusphere-2022-616
Preprint. Discussion started: 29 August 2022

Abstract. To date, knowledge on the effects of decadal-scale changes in climatic forcing on sediment export from glaciated high alpine areas is still limited. This is primarily due to the extreme scarcity of sufficiently long records of suspended sediment concentrations (SSC), which precludes robust explorations of longer-term developments. Aggravatingly, insights are not necessarily transferable from one catchment to another, as sediment export can heavily depend on local preconditions (such as geology or connectivity). However, gaining a better understanding of past sediment export is an essential step towards estimating future changes, which will affect downstream hydropower production, flood hazard, water quality and aquatic habitats.

Here we test the feasibility of reconstructing decadal-scale sediment export from short-term records of SSC and long time series of the most important hydro-climatic predictors, discharge, precipitation and air temperature (QPT). Specifically, we test Quantile Regression Forest (QRF), a non-parametric, multivariate approach based on Random Forests. We train independent models for the two nested and partially glaciated catchments Vent (98 km²) and Vernagt (11.4 km²) in the Upper Ötztal in Tyrol, Austria (1891 to 3772 m a.s.l.), to gain a comprehensive overview of sediment dynamics. In Vent, daily QPT records are available since 1967, alongside 15 years of SSC measurements. At gauge Vernagt, QPT records started in 1975 in hourly resolution, which allows comparing model performances in hourly and daily resolution (Validation A). Challengingly, only four years of SSC measurements exits at gauge Vernagt, yet consisting of two 2-year datasets, that are almost 20 years apart, which provides an excellent opportunity for validating the model's ability to reconstruct past sediment dynamics (Validation B).

As a second objective, we aim to assess changes in sediment export by analyzing the reconstructed time series for trends (using Mann-Kendall test and Sen's slope estimator) and step-like changes (using two complementary change point detection methods, the widely used Pettitt's test and a Bayesian approach implemented in the R package 'mcp').

Our findings demonstrate that QRF performs well in reconstructing past daily sediment export (Nash-Sutcliffe efficiency of 0.73) as well as the derived annual sediment yields (Validation B), despite the small training dataset. Further, our analyses indicate that the loss of model skill in daily as compared to hourly resolution is small (Validation A). We find significant positive trends in the reconstructed annual suspended sediment yields at both gauges, with distinct step-like increases around 1981. This coincides with a crucial point in glacier melt dynamics: we find co-occurring change points in annual and summer mass balances of the two largest glaciers in the Vent catchment. This is also reflected in a coinciding step-like increase in discharge at both gauges as well as a considerable increase in the accumulation area ratio of the Vernagtferner glacier. We identify exceptionally high July temperatures in 1982 and 1983 as a likely cause, as July is the most crucial month with respect to firn and ice melt. In contrast, we did not find coinciding change points in precipitation.

This study demonstrates that the presented QRF approach is a promising tool with the ability to deepen our understanding of the response of high-alpine areas to decadal climate change. This in turn will aid estimating future changes and preparing management or adaptation strategies.

1 Introduction

Sediment production rates per unit area are highest in the world's mountains (Hallet et al., 1996), headed by modern glaciated basins (Hinderer et al., 2013). As a consequence, sediments transported from these rapidly deglaciating high alpine areas have substantial effects on hydropower production and reservoir sedimentation (Schöber and Hofer, 2018; Guillén-Ludeña et al., 2018), flood hazard (Nones, 2019) as well as water quality, nutrient and contaminant transport and aquatic habitats (Gabbud and Lane, 2016; Bilotta and Brazier, 2008; Vercruysse et al., 2017) and impact global sediment and biochemical balances (Herman et al., 2021). Thus, there is considerable interest in water resource research and management to gain better understanding of sediment dynamics in high alpine areas, also to mitigate and adapt to future changes.

However, there is still limited quantitative understanding of sediment transport in high-alpine rivers and their relation to changes in climatic forcing over relevant temporal scales, i.e. at decadal and centennial scales as opposed to longer ones (Huss et al., 2017; Antoniazza and Lane, 2021; Herman et al., 2021). This is partly owed to the complexity of sediment dynamics in high-alpine areas, which are the result of an intricate system of climatic forcing and hydro-geomorphological processes (Costa et al., 2018; Vercruysse et al., 2017).

A significant body of knowledge exists on how some of the components of these complex systems have changed in recent decades due to rising temperatures. Cryospheric changes include widespread and accelerating glacier retreat (Abermann et al., 2009; Sommer et al., 2020) and reduced extent and duration of snow cover (Beniston et al., 2018; Chiarle et al., 2021). As a result, hydrological regimes are changing from glacial to nival and from nival to pluvial regimes (Beniston et al., 2018), which results in changes in water quantities (Vormoor et al., 2015; Wijngaard et al., 2016), streamflow variability (van Tiel et al., 2019) and hydrograph timing (Kormann et al., 2016; Kuhn et al., 2016; Hanus et al., 2021; Rottler et al., 2020, 2021). These hydrological changes can translate to changes in erosivity, sediment transport capacities and fluvial erosion. At the same time, sediment supply changes, as glacier retreat uncovers large amounts of sediment previously inaccessible to pluvial and fluvial erosion (Carrivick and Heckmann, 2017; Leggat et al., 2015), subglacial sediment discharge transiently increases (Costa et al., 2018; Delaney and Adhikari, 2020) and continuing permafrost thaw destabilizes slopes and facilitates mass movements (Huggel et al., 2010, 2012; Beniston et al., 2018; Savi et al., 2020). Adding to this, erosive precipitation has a higher chance of affecting unfrozen material during prolonged snow-free periods (Kormann et al., 2016; Rottler et al., 2021; Wijngaard et al., 2016).

Yet the magnitude of these impacts is catchment-specific, as it depends e.g. on the area occupied by glaciers and permafrost or basin hypsometry (Huss et al., 2017) and is thus not easily transferable from one site to another. Aggravatingly, high-alpine sediment dynamics are highly variable over time, so that long time series are required to assess systematic changes. Yet, most records are too short for such analyses and long enough data are extremely rare, especially in glaciated headwaters, which are often especially challenging to monitor.

To our best knowledge, only very few examples of decadal sediment records from the European Alps exist in the current literature. Costa et al. (2018b) report on an exceptional record of suspended sediment concentrations from the Upper Rhône basin, Switzerland, of almost five decades, albeit these recordings are severely affected by anthropogenic impacts (hydropower generation and gravel mining) and integrate over an area of 5340 km². Michelletti and Lane (2016) and Lane et al. (2017) reconstructed coarse sediment export from hydropower intake flushings at decadal scales in three small catchments in the Hérens Valley, Switzerland, however not taking into account the amount of suspended sediment transport, which is often at least as large as the amount transported as bedload (Schöber and Hofer, 2018; Mao et al., 2019; Turowski et al., 2010). Further long-term sediment records can be inferred from lake stratigraphy (e.g., Lane et al., 2019) – yet such studies are of course confined to catchments where lakes are present. To compensate for this lack of measurement data, we aim to estimate longer-term past suspended sediment dynamics based on the available shorter records of suspended sediment concentrations.

Thus, the first objective of this study is to test a quantile regression forest approach for the reconstruction of suspended sediment dynamics at decadal scales. Quantile regression forests (QRF) (Meinshausen, 2006) are a multivariate non-parametric regression technique based on random forests, that have performed favorably to sediment rating curves and generalized linear models in modelling suspended sediment concentrations (Francke et al., 2008a). As an advantage to other machine-learning approaches, QRF allow to quantify the model uncertainty (Francke et al., 2008a; Al-Mukhtar, 2019). In past studies, QRF have been successfully applied for sedigraph reconstruction in badland-dominated catchments in Spain (Francke et al., 2008a, b) and in a tropical forest in Panama (Zimmermann et al., 2012), specifically by including proxies for erosive processes, e.g. precipitation, discharge and seasonality. We adapted this approach to high alpine catchments by adding air temperature as a predictor in addition to discharge and precipitation. We then applied it to the gauges Vent Rofenache and Vernagt in a nested catchment setup in the Rofental, located in the Upper Ötztal in Tyrol Austria. The data situations at the two gauges bear different challenges and opportunities, and taken together give a good overview of sediment dynamics in this location.

The second objective of this study is to examine the resulting estimates of annual suspended sediment yields with respect to changes at decadal scales. Thus, we analyze the time series with respect to trends, which could be expected e.g. due to ongoing temperature increase. However, the possibility of sudden, tipping-point-like shifts in response to climatic changes has been suggested for cryospheric geomorphic systems (Huggel et al., 2012) and especially sediment dynamics (Vercruysse et al., 2017) and indeed a step-like increase has been observed on suspended sediment concentrations in the Rhône basin (Costa et al., 2018). Hence, we use change point detection methods to assess whether the detected trends are gradual or follow a step-like pattern. We extend this analysis to the predictors (temperature, discharge and precipitation) as well as annual mass balances to assess possible reasons for changes in suspended sediment yields.

2 Study area

The study area is located in the "Rofental", a valley in the Upper Ötztal in the Tyrolean Alps, Austria. For more than 100 years, the area has been subject to intense glaciological and hydrometeorological research , yielding outstanding data sets (Strasser et al., 2018). The entire catchment is 98.1 km² upstream gauge "Vent Rofenache" (hereafter "Vent") and nested within is the 11.4 km² catchment upstream gauge "Vernagt" (see Fig. 1). The gauge Vent is run by the Hydrographic Service of Tyrol; and Vernagtferner by the Bavarian Academy of Sciences and Humanities. The catchments' elevations range from 1891 m a.s.l. at gauge Vent and 2635 m at gauge Vernagt to the summit of Wildspitze, the highest peak in Tyrol, at 3772 m.

The study area's shielded location in the inner Alpine region leads to the relatively warm and dry climate (Kuhn et al., 1982). Mean annual temperature and precipitation at the gauge in Vent are 2.5°C and about 660 mm (Hanzer et al., 2018; Hydrographic yearbook of Austria, 2016; Strasser et al., 2018), but a considerable precipitation gradient with elevation of about 5 % per 100 m has been described (Schöber et al., 2014).

Both catchments are heavily glaciated, with approximately 28 % and 64 % glacier cover in 2015 (Buckel and Otto, 2018). The two largest glaciers within the Vent catchment, Vernagtferner and Hintereisferner have been systematically observed since the 1950s and 60s and have shown accelerating retreat since the beginning of the 1980s (Abermann et al., 2009), which is expected to continue in the future (Hanzer et al., 2018).

The catchment is drained by the river Rofenache, which flows into the Ötztaler Ache, one of the largest tributaries to the river Inn. The hydrological regime (glacial to nival) shows a pronounced seasonality as most of the discharge is fed by snow and glacier melt and about 89 % of the discharge in Vent occurs from April to September (Schmidt et al., 2022b; Hanzer et al., 2018).

The Ötztal Alps are part of the Ötztal-Stubai massif within the crystalline central Eastern Alps and the catchment geology is dominated by biotite-plagioclase, biotite and muscovite gneisses, variable mica schists and gneissic schists (Strasser et al., 2018). The land cover of higher elevations is dominated by glaciers, bare rock or sparsely vegetated terrain whereas mountain pastures and coniferous forests are present at lower altitudes.

Suspended sediment concentrations at the gauge in Vent showed to be the highest in an Austria-wide comparison (Lalk et al., 2014) and annual suspended sediment yields are about 1500 t/km² on average (Schmidt et al., 2022b). Suspended sediment dynamics showed an even more pronounced seasonality compared to discharge, as 99 % of the annual suspended sediment yields are transported from April to September (ibid.).

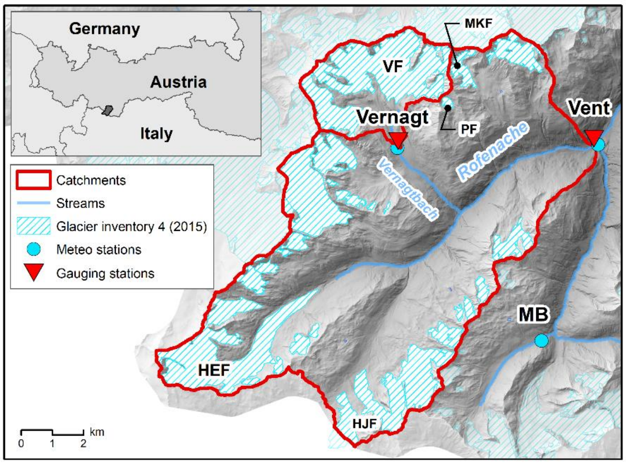

Figure 1 Map of the catchment area upstream gauge Vent and nested within the Vernagt catchment, with glaciers Vernagtferner (VF) and Hintereisferner (HEF) as well as the measurement station Martin-Busch-Hütte (MB). Smaller glaciers Hochjochferner, Platteiferner and Mitterkarferner are denoted by HJF, PF and MKF, respectively. Sources: 10 m DTM of Tyrol *(Land Tirol, 2016)*, **glacier inventory 4 (2015)** *(Buckel and Otto, 2018)*, **rivers from tiris open government data** *(Land Tirol, 2021)*.

3 Methods

In essence, we train a non-parametric model on suspended sediment concentrations and predictors (discharge, temperature, precipitation) and then use this model and long-term records of the predictors to reconstruct past suspended sediment concentrations and derive annual suspended sediment yields. We then analyze the resulting time series with respect to trends and change points.

In the following section, we will briefly describe the input data and their preparation for the model, the general idea of QRF, the construction of ancillary predictors and our modifications, the modelling structure we applied and our validations as well as the statistical tools used for the analysis of the results.

3.1 Characteristics, sources and adjustments of input data

Here we describe the input data and their preparation for modelling. Details such as coordinates of stations and gauges, the temporal resolution of the different time series, their sources and data availability can be found in table A1 in appendix A.

3.1.1 Discharge data, precipitation and temperature data

Gauge Vent has been operated continuously by the Hydrographic Service of Tyrol since 1967 (Strasser et al., 2018) and discharge has been measured through water stage recordings, complemented by a radar probe since 2000. At gauge Vernagt, discharge has been recorded since 1974 (Bergmann and Reinwarth, 1977) and is determined through water stage recordings and tracer-calibrated stage-discharge relations. Additionally, this is complemented by ultrasonic stage measurements, providing nearly uninterrupted discharge series since 1974 (Braun et al., 2007).

Precipitation and temperature have been recorded close to the gauge in Vent (see map) since 1935 and are available in daily resolution. Both time series showed gaps, which creates a problem when using the chosen QRF approach. Thus, we filled these gaps using precipitation data recorded at the Vernagt gauge (aggregated to daily sums and using a correction factor of $P_{\mathrm{Vent}} = P_{\mathrm{VF}}/1.3$ obtained from concomitant periods) and temperature data recorded at Martin-Busch-Hütte (see fig. 1) (aggregated to daily means and using a correction factor of $T_{\mathrm{Vent}} = T_{\mathrm{MB}} * 2.8089$). As a result, 2 % of the precipitation and 0.25 % of the temperature time series were filled (see fig. A1 in the appendix).

At gauge Vernagt, precipitation and temperature have been recorded in high temporal resolution next to the gauge since 1974. To fill the present gaps, we used data recorded by the Hydrographic Service since 2010 in close proximity to the Vernagt station. As some gaps still remained, we subsequently used data recorded at Martin-Busch-Hütte (conversion factors: $\mathrm{Temp}_{\mathrm{VF}} = -0.002536 \cdot \mathrm{Temp}_{\mathrm{MB}}^2 + 0.9196 * \mathrm{Temp}_{\mathrm{MB}} - 0.474$; $\mathrm{Precip}_{\mathrm{VF}} = 0.895 \cdot \mathrm{Precip}_{\mathrm{MB}}$). With this, 12 % of the precipitation time series and 9 % of the temperature time series were filled, although many of these filled gaps occur during the winter months, when the discontinued discharge data inhibit QRF modelling anyway (see fig. A1 in the appendix). Some gaps still remain, but these, too, are mostly restricted to winters. We excluded the data from 1974 from the analyses at gauge Vernagt, as data were not available for the entire year.

3.1.2 Turbidity and suspended sediment concentration data

At gauge Vent, turbidity has been measured using two optical infrared turbidity sensors (Solitax ts-line and Solitax hs-line by Hach) since 2006. To calibrate the turbidity measurements to suspended sediment concentrations (SSC), water samples are taken manually from the stream close to the turbidity sensors frequently (Lalk et al., 2014). Turbidity measurements are paused every winter (between October and April) to avoid damage to the equipment. However, the equipment is reinstalled early enough to capture the spring rise in concentrations, and winter sediment transport can be considered negligible (Schmidt et al., 2022b).

At gauge Vernagt, water is diverted into a measuring chamber (Bergmann and Reinwarth, 1977), where turbidity can be recorded while avoiding damage to the equipment by large rocks in the main channel. Turbidity was recorded in the summers of 2000 and 2001 (Staiger-Mohilo STAMOSENS 7745 UNIT) (Naeser, 2002) as well as 2019 and 2020 (Campbell OBS501). Water samples for calibration of turbidity to SSC were taken directly next to the turbidity sensor, by hand in 2000 and 2001 (57 samples), and by means of an automatic sampler (ISCO 6712) in 2019 and 2020 (131 samples). The latter initiated sampling if one of two criteria was met: (i) regular sampling, to avoid long gaps between two samples, (ii) threshold-based sampling to obtain samples across the whole range of possible turbidity values. Gravimetric sediment concentrations SSC_g were then determined in the laboratory and used to convert turbidity to SSC (2000/01: SSC [g/l] = 0.1583 * turbidity [V] $^{-13.0877}$ (Naeser, 2002); 2019/20: SSC [g/l] = 0.00212*turbidity [FNU]).

3.1.3 Aggregation/disaggregation to different temporal resolutions

As temporal resolutions varied between the different time series, we aggregated or disaggregated the data to achieve homogenous temporal resolutions for the respective QRF models in daily, hourly and 10-minute resolution.

To compute annual Q, P and T values, we computed daily Q sums derived from the available daily means (Q_{sum} [m³/day] = 60 * 60 * 24 * Q_{mean} [m³/s]), summed up daily precipitation sums and computed annual averages of daily mean temperatures. However, due to inconsistent gaps in winter temperature and precipitation measurements at gauge Vernagt, we only considered data between May 1st and September 30th of each year.

3.2. Quantile regression forests (QRF) for sedigraph reconstruction

To reconstruct suspended sediment dynamics, the desired models have to account for a multitude of processes controlling SSC (discharge dynamics, temperature-dependent activation of sediment sources and transport processes, precipitation, antecedent wetness conditions, etc.), need to deal with non-normal distributions of both predictor and response variables and have to handle correlations between the predictors (Zimmermann et al., 2012).

Quantile regression forests (QRF) (Meinshausen, 2006) represent a multivariate approach that can deal with non-linearity, interactions and non-additive behavior without making assumptions on underlying distributions, and performed favorably in reproducing sediment dynamics as compared to generalized linear models or sediment rating curves (Francke et al., 2008a). QRF are a generalization of random forests (RF) regression tree ensembles (Breiman, 2001). Regression trees (a.k.a. CARTs) (Breiman et al., 1984) apply recursive rule-based data partitioning in order to group data with similar values for the response variable (Francke et al., 2008a). RF and QRF employ an ensemble of these trees, each one grown on a random subset (bootstrap sample) of the training data. Predictive performance is evaluated on those parts of the data that are not considered in the bootstrap sample, i.e. the out-of-bag data (OOB) (ibid.). Model predictions are then obtained from the mean of predictions of each single tree (RF) or based on the distribution of these single-tree predictions (QRF). As QRF keeps the value of all observations within a node, it enables the quantification of the model uncertainty, which represents an advantage

https://doi.org/10.5194/egusphere-2022-616
Preprint. Discussion started: 29 August 2022

to other non-parametric approaches applied to SSC modelling, such as fuzzy logic or artificial neural networks (ibid.).

We built on the model setup developed by (Francke et al., 2008b; Zimmermann et al., 2012), who integrated antecedent conditions of the considered primary predictors over various aggregation periods. Extending this idea, we added temperature (and antecedent temperature conditions) to the group of predictors, as many processes determining sediment dynamics in high alpine are temperature-sensitive (i.e. the activation of sediment-rich glacial meltwaters).

Secondly, we tuned the model with respect to the length of the antecedent periods considered: To describe antecedent conditions of Q, P and T while keeping correlation between the derived predictors as low as possible, we used non-overlapping time windows of increasing sizes from the primary predictors Q, P and T (Zimmermann et al., 2012) and optimized the model performance with respect to the length of these time windows. We optimized the model results with respect to the Nash-Sutcliffe efficiency index (see section 3.2.1) in a 5-fold cross validation, that divided the training data into five equal temporally contiguous chunks.

To derive annual suspended sediment yields, we performed 250 Monte-Carlo realizations for each year which allows assessing the prediction uncertainty. From these, the mean and quartiles of annual suspended sediment yields are computed.

3.3. General modeling approach and adaptations to conditions at the two gauges

We combine the analysis of the two gauges Vent and Vernagt to gain a more reliable and comprehensive understanding of past sediment dynamics in the Rofental. In this, the data situations at the two gauges bear different challenges and opportunities.

At gauge Vent, continuous turbidity-derived SSC time series have been recorded in high temporal resolution (15 minutes) since 2006, providing abundant training data for our model. Additionally, the long-term predictor data are available back until 1967, facilitating insights into long-term developments - yet only in daily resolution, which predetermines the temporal resolution of the reconstruction model. This is challenging as sediment concentrations vary considerably during one day, leaving us with the need to assess whether a daily model adequately represents sediment dynamics.

At gauge Vernagt, the availability of hourly discharge (Q), precipitation (P) and temperature (T) data back until 1974 is truly remarkable. Yet, turbidity-derived SSC data have only been recorded for the years 2000, 2001, 2019 and 2020 (see Fig. 2, upper panel "Vernagt", left side, plots labelled "SSC"). Additionally, the data in 2019 and 2020 are affected by episodic siltation and periods when the turbidity sensor reached saturation: 0.47 % of the two summers of data were affected by saturation and about 8 % were affected by siltation. The latter was mainly due to one period of about 16 days in August 2019. Additionally, there were three shorter incidents (1.5 hours to 1.5 days), two in 2019 and one in 2020. These issues first need to be dealt with in order to provide accurate training data for our model, as it is sensitive to the range of values represented in the training data (Francke et al., 2008a). On the other hand, the 16-year gap between the measurement periods provides the extraordinary opportunity to verify the model's skill in reconstructing past SSC against real measurement data.

To address these issues and benefit of the opportunities, we preformed three preparatory steps before the final reconstruction models (fig. 2):

1. **Gap-filling model:** At gauge Vernagt, we trained a model on SSC determined from 131 water samples and the predictors (Q, P, T) in the highest possible (i.e. 10-minute) resolution (fig. 2, upper panel). We used the resulting modelled SSC to replace periods in the 2019/20 SSC data that were affected by siltation or sensor saturation. As the sampling scheme was customized to cover hydro-sedimentological conditions as widely as possible (see Schmidt et al., 2022), the water samples also partially cover the periods to be addressed by the gap filling.
2. **Validation A - temporal resolution:** we ran models in both hourly and daily resolution at gauge Vernagt to assess the error magnitude due to the coarser temporal resolution.
3. **Validation B – extrapolation:** we trained a model on the repaired Vernagt SSC data of 2019 and 2020 and reconstructed SSC back until 2000 for validation against the 2000/01 measurement data (fig. 2, center).

Third, we ran the final ‘reconstruction models’, taking into account all available training data to reconstruct SSC back until 1967 and 1974, respectively.

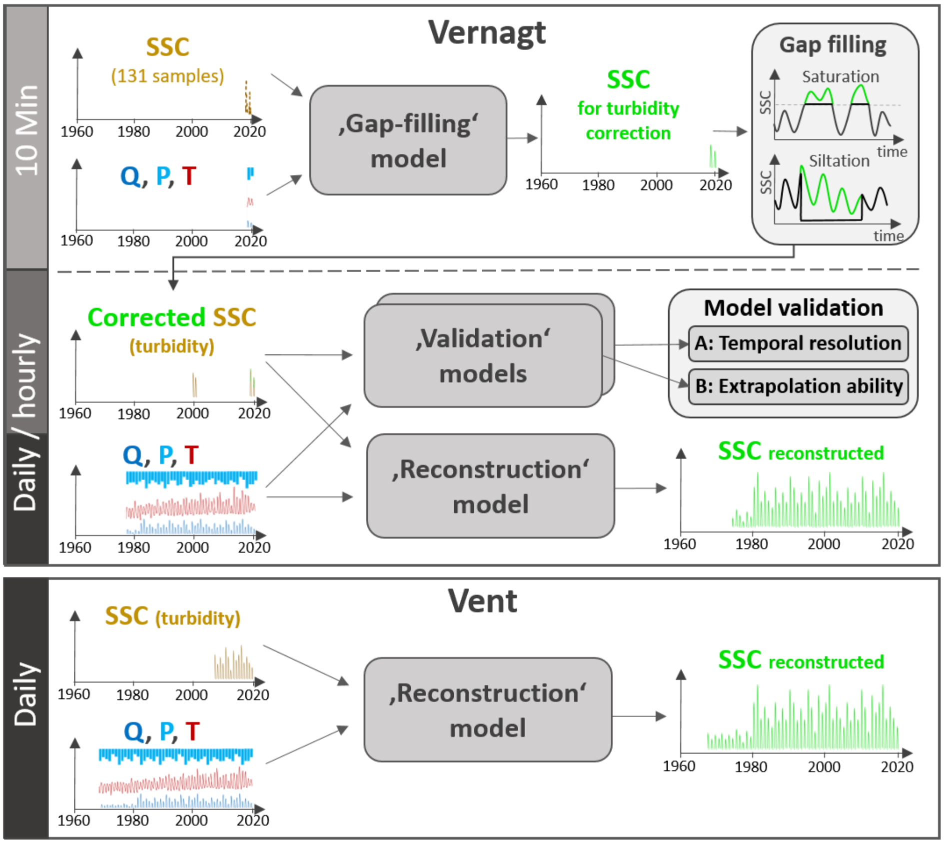

Figure 2: Overview of modelling approach. SSC = suspended sediment concentration; Q = discharge; P = precipitation; T = temperature.

3.2 Analysis of results

3.2.1 Units, conversions and quality measures

From suspended sediment concentrations (SSC, modelled and from turbidity) and discharge (Q), we calculated sediment discharge Q_{sed} [t/time] (for analyses in high temporal resolution), daily q-weighted SSC averages SSC_{daily} [kg/m³] (to account for the very skewed nature of SSC in aggregating to daily resolution), annual suspended sediment yields SSY [t/a] and specific annual suspended sediment yields sSSY [t/a/km²] (for comparability among the gauges) as follows:

$$Q_{sed}(t) = SSC(t) \cdot Q(t), \qquad (1)$$

where Q is discharge [m³/s],

$$SSC_{daily} = \frac{\Delta t \cdot \sum Q_{sed}(daily)}{\Delta t \cdot \sum Q(daily)}, \qquad (2)$$

where Δt is the corresponding temporal resolution [s],

$$SSY = \Delta t \cdot \sum Qsed \text{ , and} \qquad (3)$$

$$sSSY = \frac{SSY}{A}, \qquad (4)$$

where A [km²] is the catchment area.

To quantify model performance and for our validation, we used the Nash-Sutcliffe efficiency index:

$$NSE = 1 - \frac{\sum_{i=1}^{n}[SSC_{obs}(i) - SSC_{mod}(i)]^2}{\sum_{i=1}^{n}[SSC_{obs}(i) - \overline{SSC_{obs}}]^2}, \qquad (5)$$

where 'obs' and 'mod' refer to observed and modelled SSC values and $\overline{SSC_{obs}}$ is the mean of observed SSC values (Zimmermann et al., 2012). However, sediment export in the study area is highly seasonal (see also Schmidt et al., 2022) so that the NSE might be misleading, as models reproducing seasonality but fail to reproduce smaller fluctuations can still report a good NSE value (Schaefli and Gupta, 2007). Thus, we additionally computed the normalized benchmark efficiency as follows:

$$BE = 1 - \frac{\sum_{i=1}^{n}[SSC_{obs}(i) - SSC_{mod}(i)]^2}{\sum_{i=1}^{n}[SSC_{obs}(i) - SSC_{bench}(i)]^2}, \qquad (6)$$

where SSC_{bench} refers to the benchmark model suspended sediment concentration at timestep i. Commonly, this benchmark model is the mean of the observations for every Julian day over all years within n (i.e. the mean annual cycle) (see, e.g., Pilz et al., 2019). However, this is heavily influenced by individual events in our case, so we used the 60-day moving average of the mean SSC for every Julian day instead.

3.2.2 Methods for trend analysis and change point detection

In order to quantify time series behavior, we generally followed the approach of first analyzing for existence of a trend. If a trend was detected, we assessed whether the trend was homogenous by analyzing for change points. If a change point was identified, we then examined the resulting segments of the time series for trends.

Most of the investigated time series are not normally distributed and some show autocorrelation. Thus, to calculate trend significance, we used the non-parametric Mann-Kendall test for linear trend detection in a version that was modified to detect trends in serially correlated time series (Yue and Wang, 2004) as recommended by (Madsen et al., 2014). To estimate trend magnitude, we used Sen's slope (SS) estimator (Sen, 1968). Both methods are implemented in the "mkTrend" function of the R-package "FUME" (Santander Meteorology Group, 2012). In our

https://doi.org/10.5194/egusphere-2022-616
Preprint. Discussion started: 29 August 2022

results, we only plot and refer to trends that were significant at least at a significance level $\alpha = 0.05$ after correction for autocorrelation.

For change point detection, we used the non-parametric Pettitt's test (Pettitt, 1979), which is commonly used as it is a powerful rank-based test for a change in the median of a time series and robust to changes in distributional form (Yue et al., 2012), as implemented in the R package "trend" (Pohlert, 2020). However, it only gives one change point location without uncertainty quantification around its location and was shown to be sensitive to the position of the change point within the time series, i.e. detection at the beginning and end of the series is unlikely (Mallakpour and Villarini, 2016).

Thus, as a complementary advanced approach, we used Bayesian regression with change points as implemented in the R-package "mcp" (Lindeløv, 2020). This represents a much more flexible approach and allows to asses uncertainty through the resulting posterior distributions of the change point location. Although mcp allows to detect multiple change points, we only considered one change point as we aimed to detect the largest shift in the time series and to ensure comparability with Pettitt's test. Unless specified otherwise, we used the uninformative default prior, allowed free slope estimation before and after the change point, assumed a disjoined slope (i.e. step-like change) at the change point and allowed for changes in variance at the change point.

As mentioned earlier, we computed 250 Monte-Carlo realizations of the annual SSY as a result of the QRF model. We propagated this uncertainty by applying the trend and change point detection methods not only to the mean estimates but also to the 250 resulting time series realizations.

All calculations were done in R, version 4.2.1 (R Core Team, 2018).

4. Results Part I – Model evaluation

4.1. Validation A: Influence of reduction of temporal resolution

As described earlier, the temporal resolution for long-term reconstruction is limited to daily, as the respective predictor data are available only in daily resolution. As a result, we can expect some loss of information that can be crucial for sediment dynamics, such as short-term precipitation intensity. To assess the error magnitude, we ran two variants of the models at gauge Vernagt, in daily and hourly resolution based on all available training data (i.e. 2000, 2001, 2019 and 2020). We then compared daily sediment discharge (Q_{sed}) calculated from the out-of-bag model estimates to Q_{sed} calculated from measured turbidity (fig. 3a). Both models reproduce daily Q_{sed} very well, where the daily model shows a larger scatter, which is also reflected in the slightly lower NSE and BE. The comparison of annual sSSY (fig. 3b) shows very similar estimates in most years.

As the loss of model skill and difference between the two model results are small, we use the daily resolution models at both gauges in the following analyses for better comparability and applicability to the full length of the time series.

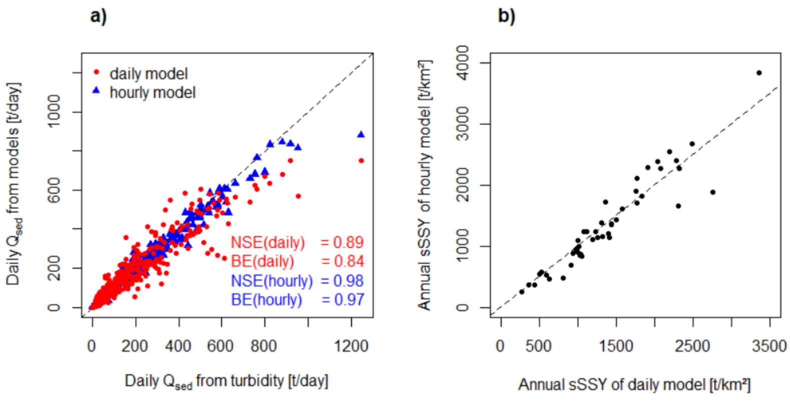

Figure 3: a) Daily Qsed calculated from out-of-bag prediction of daily and hourly models vs. Qsed calculated from turbidity at gauge Vernagt; b) Comparison of mean annual sSSY estimates of the daily and hourly models at gauge Vernagt. NSE: Nash-Sutcliffe-efficiency; BE: benchmark efficiency.

4.2. Validation B: Capability of temporal extrapolation

To evaluate the capability of the QRF models to reconstruct past SSC, we trained a daily model on the 2019/20 (n = 212) data at gauge VF and used the data of 2000/01 (n = 367) for validation. The comparison of Q_{sed} determined from turbidity to modelled Q_{sed} shows that the model underestimates high daily Q_{sed} (fig. 4 a). Nevertheless, the NSE of 0.73 and BE of 0.66 are indicative of a good representation of sediment dynamics in daily resolution. Annual yields are affected by overestimation in late August 2000 and underestimation in July 2001 (fig. 4 b). As a result, the mean annual sSSY estimates are 31 % higher and 16 % lower than observed annual sSSY in 2000 and 2001, respectively. Considering the spread of the model results (i.e., the 2.5 and 97.5 percentiles of the 250 model predictions as depicted by the whiskers in fig. 4 b), 19 % overestimation compared to the maximum model estimate in 2000 and 4 % underestimation compared to the minimum model estimate in 2001 remain.

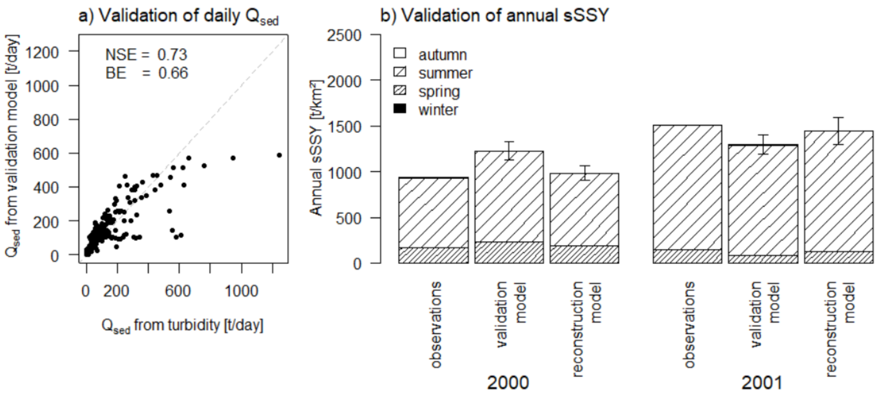

Figure 4: a) Daily modelled Qsed from the validation model versus Qsed from turbidity for the years 2000 and 2001 at gauge VF. b) Annual sSSY based on turbidity observations, estimates of the validation model (without 2000/01 data) and estimates of the reconstruction model (all training data) in 2000 (left) and 2001 (right). Subdivision into seasons: spring (bottom, Apr – Jun), summer (middle, Jul – Sep), autumn (top, Oct – Dec). Boxes depict mean model estimates and whiskers depict 2.5 and 97.5 percentiles of model predictions. NSE: Nash-Sutcliffe-efficiency; BE: benchmark efficiency.

4.3. Exceedances of predictor ranges in the past

It is a known limitation of QRF that it is not possible to extrapolate beyond the range of values represented in the training data. For example, if the discharge measured on a day in the reconstruction period (Q_{rec}) exceeds the maximum discharge within the training period ($Q_{train,\ max}$), the model potentially cannot make a reliable prediction of SSC on that day. Therefore, we need to assess whether and how often the ranges of the predictors in the training data were exceeded during the reconstruction period.

At gauge Vent, maximum Temperature of the training period ($T_{train,\ max}$) was not exceeded during the reconstruction period. $Q_{train,\ max}$ was overstepped on 4 days in 1987 and precipitation within the reconstruction period was larger than the maximum precipitation during the training period ($P_{train,\ max}$) on 3 days within the reconstruction period.

At gauge Vernagt, $Q_{train,\ max}$ was exceeded 6 times in the reconstruction period, and 4 of these days occurred in 2003. There was one day at gauge Vernagt, were $T_{train,\ max}$ was exceeded in 2017. $P_{train,\ max}$ was exceeded on 5 days within the reconstruction period, however on 2 of these days, the temperature was below zero and discharge was very low, so we consider these days negligible for annual sediment export.

There were also days at both gauges when discharge was lower than the minimum discharge measured discharge during the training period ($Q_{train,\ min}$). Yet all of these days were in April, May or October, when SSC are very low, and as very low discharge also translates to very low transport capacities, we consider the error negligible for annual sediment yields.

4.4. Performance of the reconstruction models

To test the performance of the reconstruction model in Vent, we plotted daily out-of-bag Q_{sed} predictions and Q_{sed} from turbidity (fig. 5a) as well as modelled and measured annual sSSY (fig. 5 b). This shows that rare days with extremely high Q_{sed} (above ca. 7000 t/day) are systematically underestimated. The NSE of modelled vs. measured Q_{sed} of 0.64 represents a satisfactory performance (n = 2760) as does the BE of 0.54. This is much lower than the NSE of 0.89 and BE of 0.84 of the daily model at gauge Vernagt (fig. 3a). Nevertheless, with respect to annual estimates, the NSE of modelled sSSY vs. sSSY derived from turbidity of 0.83 show very good agreement (fig. 5 b).

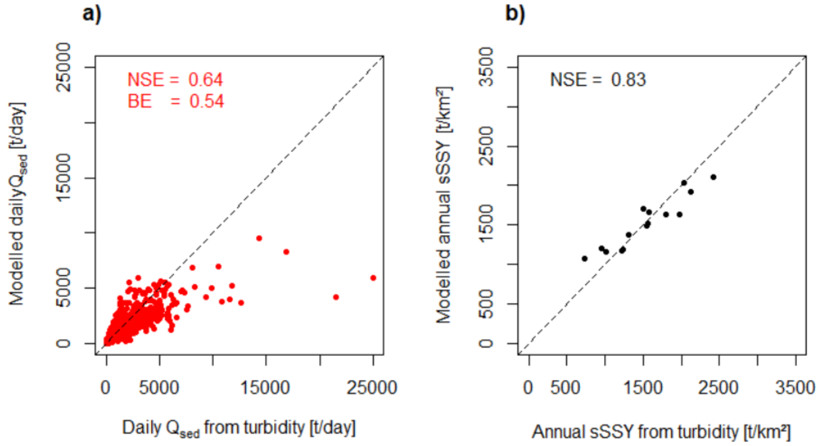

Figure 5: a) Daily Qsed calculated from out-of-bag prediction of model vs. Qsed calculated from turbidity at gauge Vent; b) Comparison of mean modelled sSSY and measured annual sSSY at gauge Vent. NSE: Nash-Sutcliffe-efficiency; BE: benchmark efficiency.

5. Results – Part II: Analysis of time series of annual sSSY estimated by QRF model

5.1. Annual sSSY and their development over time

In the resulting time series, the average sSSY of all years (± 1 standard deviation) is 1401 (± 453) t/km/yr at gauge Vent and 1383 (± 668) t/km/yr at gauge Vernagt. This indicates overall similar magnitudes of sediment export per catchment area, yet with much higher variability at gauge Vernagt. To assess how suspended sediment dynamics changed over time, we analyzed the time series of annual sSSY at the two gauges for trends and change points.

At both gauges, mean modelled annual sSSY show significant positive trends (fig. 6). In Vent, 97.6 % of the 250 time series realizations show significant positive trends (Sen's Slope (SS): 9 – 15 t/km²/a) and at VF, all realizations show significant positive trends (SS: 28 – 35 t/km²/a).

At gauge Vent, Pettitt's test yields a significant change point in 1981 in annual sSSY, which is also true for 99.6 % of the realizations (for 1 realization, the change point was detected in 1980). Accordingly, the mcp analysis shows a rather narrow probability density distribution around 1980/81 for all realizations with maximum probability density in 1981.

At gauge Vernagt, mcp shows very similar probability density distributions to that of Vent with maximum probabilities in 1981 for all realizations. However, Pettitt's test detects a change point in 1989 ($p < 0.01$; 66 % of realizations in 1989 and 27 % in 2002). As we elaborate in the discussion, this is likely due to a limitation of the Pettitt's test. Thus we divided both time series in 1981 to examine the resulting segments for trends.

In the first segment, no significant trends were detected at gauge Vernagt, and at gauge Vent, only two of the 250 realizations show significant positive trends (SS of 11.1 and 3.9 t/km²/a; see fig. 5). In the second segment (i.e. after 1981), we detected a negative trend in mean annual sSSY at gauge Vent (SS = - 7.6 t/km²/a), as well as in 42 realizations (SS of - 13.1 to - 5.9 t/km²/a). In contrast, at gauge Vernagt mean sSSY (SS = 23.5 t/km²/a) as well as 248 of the realizations (SS of 20.2 to 27.9 t/km²/a) show strong positive trends. The average sSSY (± 1SD) of all years after 1981 is 1579 (± 391) at gauge Vent and 1537 (± 603) at gauge Vernagt.

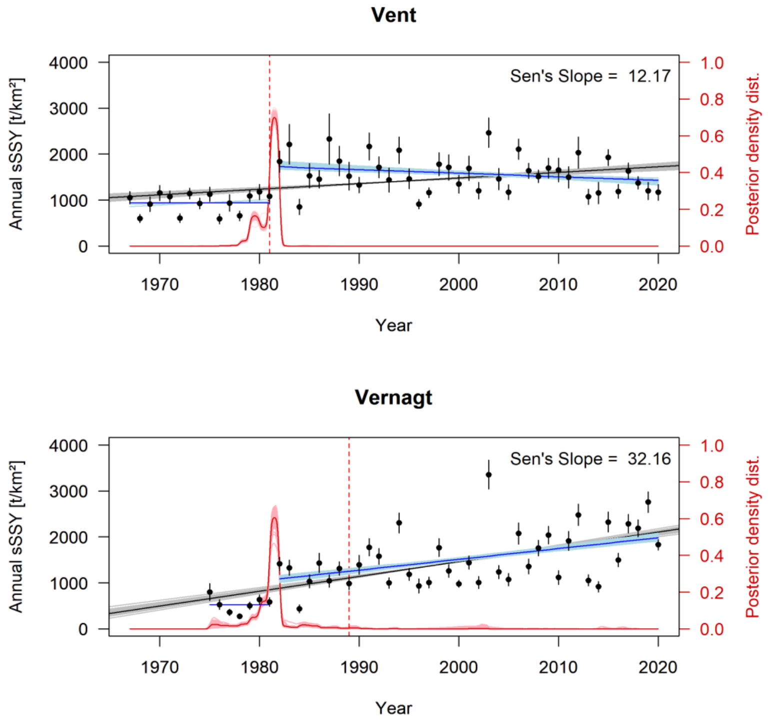

Figure 6: Mean specific annual suspended sediment yields (sSSY) as reconstructed by the QRF model (black points). Whiskers depict 2.5 % and 97.5 % quantiles of the 250 QRF realizations. Overall trend of mean annual sSSY is given by Sen's Slope (black line) and trends of all 250 QRF realizations in grey. Change points determined by Pettitt's test (red dashed line) and mcp (posterior distributions of 250 realizations as solid light red and mean as dark red lines). Trends in the time series segments before and after 1981 are given as dark blue (mean) and lightblue (realizations) lines (only plotted if significant).

5.2. Results – Part III: Analysis of predictors and other variables

We found positive trends in annual sSSY at both gauges with high probabilities of a step-like increase around 1981. To assess whether this coincides with changes in temperature (i.e. changes in snow and / or glacier melt and discharge) or changes in precipitation, we analyzed time series of temperature, discharge, glacier mass balances and precipitation with respect to trends and change points.

We derived mean annual temperatures at gauge Vent, however, at gauge Vernagt, we computed mean summer temperatures (between May and September) instead, as temperatures are missing in winter in many years (see also fig. A1 in the appendix). Both timeseries show significant positive trends but no clear change points, as Pettitt and mcp disagree and mcp yields very widespread probability distribution (fig. 7 a) and b). Additionally, we analyzed mean monthly temperatures over time and found that while most months show positive trends, at both gauges July is the only month with a high change point probability around 1981 (fig. 7 a) and b). At both stations, July temperatures in 1982 and 1983 were exceptionally warm.

Annual specific discharge sums at both gauges show significant positive overall trends (fig. 7 c) and d). In Vent, both change point detection methods indicate high probabilities of a change point in 1981. At gauge VF, the two methods disagree as in the case of annual sSSY, as the Pettitt test detects a change point in 1990 while mcp suggests a change point with high probability in 1981. Dividing both time series in the year 1981, both segments of the Vent time series show insignificant trends, while both segments at gauge VF show significant positive trends (1st segment: Sen's slope = 32.7 mm/a, $p < 0.01$; 2nd segment: Sen'S slope = 17.2 mm/a, $p < 0.001$).

We analyzed mean monthly discharge volumes and found significant positive trends in May and June in Vent. As with temperature, July was the only month where a change point was indicated by both methods, which was also in 1981. At gauge Vernagt, we detected significant positive trends from May through August and found that discharge volumes roughly doubled within the examined period, from ca. 1250 mm to ca. 2500 mm. In June, a change point was indicated around 1995 by both methods and in July, mcp indicates a CP around 1981, but the Pettitt's test did not yield a significant change point. Dividing both discharge time series in 1981, we only find a significant trend in the time after 1981 at gauge Vernagt (SS = 17.2). At gauge Vent, there is not significant trend after 1981 and Sen's Slope during this time is close to zero (SS = 0.25).

In addition to the hydro-climatic predictors considered in the QRF model, we analyzed annual mass balances of the Vernagtferner (VF) and Hintereisferner (HEF), the two largest glaciers in the Vent catchment with long mass balance records (World Glacier Monitoring Service, 2021) (fig. 7 e) and f). Annual mass balances of both glaciers show significant negative trends. Significant change points are indicated in 1985 for both glaciers by the Pettitt test, while mcp attributed (much) higher probabilities for change points to the year 1981. Notably, annual mass balances of both glaciers are almost exclusively negative after 1980 (with the exception of 1984, where mass balances are barely positive). Dividing the time series in 1981, no significant trends are detected in the first segments of both time series and significant negative trends in the second segments (HEF: -20 mm/a; VF: -17 mm/a).

Summer mass balances were only (continuously) available for the Vernagtferner and show a strong negative trend and both Pettitt and mcp detect change points in 1981 (figure 7 f). No significant trends were detected in the resulting time series segments. Winter mass balances did not show a significant trend nor change points.

Summer precipitation sums (May – September) at gauge Vent (fig. 7 g) show no significant trend, while annual precipitation sums show a significant positive trend. A change point is identified by the Pettitt's test in 1991 ($p < 0.001$) while mcp yields a widespread probability distribution with the highest probability in the late 1990s. At gauge Vernagt, we confined the analysis to summer precipitation (May – September) as the time series is affected by gaps in some winters (see fig. A1 in the appendix). Summer precipitation at gauge Vernagt shows a significant positive trend (fig. 7 h). Pettitt's test yields a significant change point in 1992 while mcp gives a very widespread distribution.

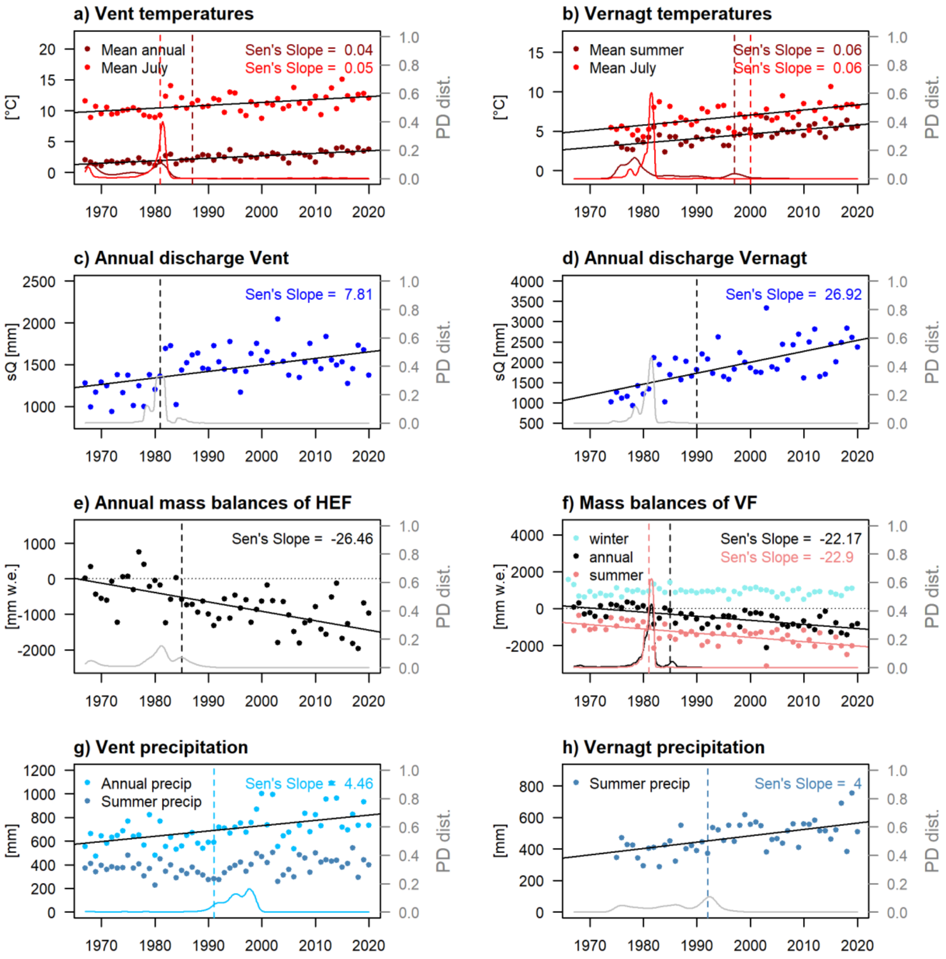

Figure 7: a) Mean annual and July temperatures in Vent; b) Mean summer (May – Sept) and July temperatures at gauge Vernagt; c) and d) annual discharge yields at gauges Vent and Vernagt; e) Annual mass balances of the Hintereisferner (HEF); f) annual, winter and summer mass balances of Vernagtferner (VF); g) Annual and summer (May – Sept) precipitation in Vent; h) Summer (May – September) precipitation at gauge Vernagt. Dashed vertical lines show change point locations according to Pettitt's test and solid lines show Sen's Slope. Both are only drawn if they are significant at α = 0.01. Lines at the bottom show posterior density distributions of mcp change point locations, with colors corresponding to the respective variables, if several variables are depicted within one plot.

6. Discussion

In the following, we will briefly summarize the most important results, before we discuss weaknesses and strengths of the presented work and integrate the results in the broader context of the literature.

In our model evaluation, we found that QRF models in reduced temporal resolution (daily as compared to hourly) still produced satisfactory results (validation A) and performed well in reconstructing past Q_{sed} and sSSY (validation B). In the reconstructed time series of annual sSSY, we detected positive trends at both gauges with high probabilities of step-like changes around 1981. This coincides with a critical point in the mass balances of the two largest glaciers in the catchment area, as well as high change point probabilities in discharge volumes and July temperatures at both gauges. With respect to precipitation, we found some positive trends but no clear change points. In the time after 1981, we found opposing trends at the two gauges, with decreasing sSSY at gauge Vent and increasing sSSY at gauge Vernagt.

6.1. Part I: Model evaluation

We found that extraordinarily high daily Q_{sed} are underestimated by our models at both gauges (figures 3 – 5), which is a little more pronounced in the daily model as compared to hourly resolution (fig. 3 a). This is not surprising given that these events are rare and figures 3 to 5 show out-of-bag predictions, which means that the respective estimates are based on trees that have seen even fewer or none of these conditions. Especially in Validation B, the validation model was trained on very few data. As another aggravating factor, the aggregation of precipitation and discharge to daily values involves some loss of information e.g. on sub-daily precipitation intensity and maximum discharge, which very likely affect sediment export. Yet as Validation A showed, this loss of information is relatively small (fig. 3 a). Additionally, this underestimation at the daily scale does not seem to propagate to annual estimates, as high annual sSSY are not systematically underestimated to the same extent (fig. 5b).

The second validation (Validation B, where we trained a model on the data of 2019/20 and compared the estimates to measurements in 2000 and 2001; fig. 4) showed over- and underestimation of annual sSSY by 31 % and 16 %, respectively. In interpreting these results, it has to be considered that the amount of data used for training is very small and less than half of the final reconstruction model (212 of 579 days), while the amount of training data is known to be crucial in data-driven models (e.g. Vercruysse et al., 2017). Especially, turbidity recordings only started in mid-July 2019, so that only one spring season was available for training. Thus, given the rigorousness of this test as well as the temporal distance of 20 years, we find that the validation yields satisfactory results with good agreement of dynamics on short timescales as well as annual estimates. However, this validation also demonstrates that the spread of the QRF model results needs to be interpreted as a minimum estimate of uncertainty, as it can only reproduce the “known unknown”, i.e. the variability represented in the training data and respective relationships.

Compared to model performance in VF with an NSE of 0.73, Vent showed a lower NSE of 0.64, which still corresponds to a satisfactory performance (Moriasi et al., 2007). We suggest that there are several reasons for this. Firstly, the Vent catchment is much larger (almost 100 km²) than the 11.4 km² Vernagt catchment. Thus, suspended sediment dynamics at gauge Vent integrate over more processes, which adds to the complexity. Secondly, precipitation measurements at gauge Vent are unlikely to be representative of the entire catchment, due to the catchment size and especially due to topographical effects. And thirdly, concentrations reach much higher values than at gauge Vernagt, so that uncertainties in the turbidity measurement are more relevant: at low concentrations, the light emitted by the turbidity sensor is predominantly scattered by solid particles, while at high concentrations, absorption becomes the dominant process. This causes the relation between the light detected by the photo sensor in the turbidity probe and SSC to become non-linear (Merten et al., 2014) and leads to a much higher variance in the SSC-turbidity relationship. However, despite these effects and the lower NSE with respect to daily Q_{sed}, annual sSSY show very good agreement.

A known limitation of QRF is the inability to extrapolate beyond the range of values represented in the training dataset. However, the total number of days when the ranges of the predictors in the training data were exceeded is very small (seven days at gauge Vent and 10 days at gauge Vernagt), so we consider the error negligible for annual sediment export. More generally, the model can only reproduce the quantitative and qualitative conditions as represented within the training data. So for example, major qualitative changes in the functioning of the system, such as changes in connectivity e.g. through the formation of proglacial lakes or large-scale storage of sediments along the flow paths, would not be captured. However, such major changes are at least not indicated in historic aerial images (Laser- und Luftbildatlas Tirol, 2022) and the longitudinal profile of the major water courses are very steep, which precludes significant sediment storage.

6.2. Part II: Analysis of time series of annual specific suspended sediment yields (sSSY)

The overall magnitudes of annual yields at two gauges fall at the high end compared to an extensive collection from the European Alps (Hinderer et al., 2013) and are in good accordance with yields from other catchments in the Stubai and Ötztal Alps (Schöber and Hofer, 2018; Tschada and Hofer, 1990) (see also Schmidt et al., 2022).

In our analysis of reconstructed annual sSSY at the two gauges, the two change point detection methods did not agree at gauge Vernagt: mcp yielded high change point probabilities around 1981, whereas the Pettitt's test detects a significant change point in 1989 and 2002. Similarly, results do not agree for July temperatures and discharge at gauge Vernagt. We attribute this to a limitation of Pettitt's test, which is known to be much less sensitive to break points located near the beginning or end of the time series (Mallakpour and Villarini, 2016). We proceed on the assumption that there is a high probability of break points around 1981 in the reconstructed sSSY as well as discharge and July temperature time series at gauge Vernagt, as the mcp probability distributions are very narrow and similar to the corresponding probability distributions in Vent.

A question to be considered is whether the detected change points are credible or e.g. due to measurement errors. Since they were detected at the two gauges independently, we deem it unlikely that e.g. a change in measurements caused the change points. Furthermore, a very similar step-like increase in measured SSC has been reported in the upper Rhône basin in Switzerland (Costa et al., 2018), only slightly later (around 1985), which is likely due to lower average temperatures in the Rhône basin as compared to the upper Ötztal. The authors attributed this shift to a step-like increase in mean annual temperature, which lead to enhanced ice melt, reduced snow cover and snowmelt contributions. They concluded that the onset of increased ice melt played a dominant role in the SSC increase, which matches the expectation that phases of glacier retreat (and re-advance) lead to the highest increase in sediment yield across glacial cycles (Antoniazza and Lane, 2021), which has been confirmed by several studies (Lane et al., 2017, 2019; Micheletti and Lane, 2016).

Our results suggest that in the Rofental, the step-like increase in sSSY reconstructed by our models is linked to the onset of increased ice melt as well, as we will discuss in section 6.3.

Interestingly, we found opposing trends in the time after 1981, with strongly increasing annual sSSY at gauge Vernagt and decreasing sSSY at gauge Vent. To some extent, this is mirrored to changes in discharge, where we found no significant trend (and Sen's slope close to zero) after 1981 at gauge Vent, but a strong positive trend at gauge Vernagt. Altogether, this could indicate a stabilization or compensation of the larger Vent catchment as opposed to the nested Vernagt catchment. This is not implausible: For example, the glacier tongue of the Hochjochferner (denoted as "HJF" in fig. 1), located in the southernmost tributary valley to the Rofental has retreated by about 2 km since the 1970s (determined based on historic aerial image collection of the State of Tyrol (Laser- und Luftbildatlas Tirol, 2022) and has now retreated behind a rock sill. Additionally, several small lakes have formed in the glacier foreland that likely act as sediment sinks. Beyond that, another two smaller glaciers in the North-Eastern part of the Vent catchment, Mitterkarferner and Platteiferner ("MKF" and "PF" in fig. 1), have disappeared almost completely since the 1970s. Conversely, the Vernagtferner glacier has also experienced considerable loss in area and volume, but lacks such pronounced qualitative changes.

6.3. Part III: Analysis of predictors

Mean annual temperature in Vent and mean summer temperature at gauge Vernagt at both locations show gradual positive trends but we do not find evidence for a clear change point. However, mean July temperatures show high change point probabilities around 1981 at both locations, which is probably heavily influenced by the extraordinarily high temperatures in July 1982 and 1983. High temperatures in July are especially relevant for firn and glacier melt, since July is the month with the highest firn and ice melt contribution to discharge, after snow melt contributions have peaked in June and snow cover has decreased substantially (Kormann et al., 2016; Weber and Prasch, 2016; Schmieder et al., 2018; Schmidt et al., 2022b).

This is also reflected in the mass balance time series of the Hintereisferner and Vernagtferner, which are almost exclusively negative after 1980, with very negative summer mass balances in 1982 and 1983. Escher-Vetter (2007) and Abermann et al. (2009) have also shown that mass loss started in 1981 at both glaciers, resulting from negative summer balances. With respect to the Vernagtferner, the drastically higher ablation area ratio of almost 80 % in 1982 as compared to around 25 % in the preceding years (Escher-Vetter and Siebers, 2007) indicates that large areas of the glacier became snow-free in 1982. This entails crucial changes in albedo and therefore intensified ice melt and thinning of firn areas due to rising energy absorption at the glacier surface (Escher-Vetter, 2007; Braun et al., 2007). We interpret this as a regime shift as summer mass balances continue to be lower than before 1981 although (July) temperatures decrease again, with the exception of 1984, which was characterized by a relatively high number snowfall days during the ablation period (Escher-Vetter and Siebers, 2007).

This shift in glacier melt is mirrored in discharge, which shows step-like increases around 1981 at both gauges and continues to be elevated after the change point. The analyses of monthly discharge showed that July was the only month with a change point around 1981 at both gauges, which again emphasizes the dominance of increased firn and ice melt. In contrast, we did not find evidence for a change in precipitation sums around 1981, which would indicate that enhanced hillslope erosion on snow- or ice-free surfaces played a crucial role in the sSSY increase. With regard to suspended sediment dynamics, it is conceivable that the increase in ice melt translates to an increase in sediment-rich glacier meltwater (Delaney and Adhikari, 2020) as well as intensified fluvial erosion of sediment-rich proglacial areas.

6.4. Outlook

The presented study demonstrated that quantile regression forest is a suitable method for estimating past sediment export, given the availability of sufficient SSC measurements for training and sufficiently long records of the predictors. Thus, it represents a promising tool with the ability to broaden our understanding of the response of high-alpine areas to climate change in the past decade. What is more, this study highlights the added value of change point identification in addition to trend analyses in the respective time series, which visualizes sudden changes in the analyzed systems and thus facilitates a better understanding of critical time periods. Future studies could help gain more knowledge on decadal-scale sediment export from high alpine areas by applying the presented approach to other catchments. In turn, advancing knowledge on past changes will support and prepare the development of management and adaptation strategies.

7. Conclusions

The lack of sufficiently long measurement records of suspended sediment concentrations (SSC) has resulted in a gap of knowledge on decadal-scale sediment export and its response to past climatic changes as opposed to longer (geological) and shorter timescales. Here, we present an attempt to compensate for this lack of measurement data by estimating past suspended sediment concentrations (SSC) from recent SSC measurements and long time series of the most important hydro-climatic variables (discharge, precipitation and air temperature) by means of a quantile regression forest model. Our validations showed that the model performs well in reproducing past sediment dynamics. Limitations include the underestimation of days with extremely high SSC, which are less frequently represented in the training dataset. However, this does not seem to affect annual sediment yields to the same extent. As a more general limitation, QRF cannot extrapolate beyond the range of values represented in the training data, but the number of days where this becomes problematic is limited in our case, because of the large and sufficiently varied dataset.

We analyze the resulting annual specific suspended sediment yields (sSSY) with respect to trends and change points. At both gauges independently, annual sSSY show positive trends as well as step-like increases after 1981. As this coincides with exceptionally high July temperatures in 1982 and 1983, distinct changes in the glacier mass balances of the two largest glaciers in the catchment area and a sudden increase in ablation area of one of the glaciers, we conclude that temperature-driven enhanced glacier melt is responsible for the increase in sSSY. This is also mirrored in discharge measurements at both gauges, which, show change points around 1981 as well. These findings also demonstrate the importance of assessing change points in addition to trend analyses, in order to detect shifts in geomorphic systems. The presented approach can provide a helpful tool for estimating past sediment dynamics in catchments where long enough SSC measurement series are lacking. This can aid in gaining more knowledge on sediment export on decadal scales, which to date is still limited, as well as prepare management and adaptation strategies to future changes.

Code availability

The code of the Quantile Regression Forest model including the preprocessed data and raw model results is available on B2Share (Schmidt et al., 2022a).

Data availability

See column ‘data availability’ in table A1 in Appendix A.

Author contribution

LKS developed the general idea and conceptualized the study with TF and PG, with mentoring and reviewing of AB. LKS gathered the raw data. LKS, PG and TF installed and maintained the automatic water sampler, for gauge Vernagt heavily supported from the installations run by CM, who also supplied past data. PG prepared the input data, adapted and extended the model code and performed modelling experiments with support and supervision of TF and LKS. LKS conducted the statistical analyses with support by TF. CM reviewed and evaluated the results

in the glaciological context. LKS prepared the original draft including all figures, and all authors contributed to writing of this paper.

Acknowledgements

This research has been supported by the Deutsche Forschungsgemeinschaft Research Training Group "Natural Hazards and Risks in a Changing World" (NatRiskChange GRK 2043/1 and GRK 2043/2 grants) as well as a field work fellowship of the German Hydrological Society (DHG).

We acknowledge the support of the Hydrographic Service of Tyrol, Austria, for providing data as well as logistical support and fruitful discussions.

We thank Oliver Korup for his encouraging advice on statistical analyses, Matthias Siebers, Andreas Bauer, Irene Hahn, Theresa Hofmann, Marvin Teschner, Nina Lena Neumann and Joseph Pscherer for their help and support during field and laboratory work as well as Stefan Achleitner, Carolina Kinzel and the Environmental Engineering laboratory at the University of Innsbruck for their kind support during field and laboratory work.

Competing interests

The contact author has declared that none of the authors has any competing interests.

References

Abermann, J., Lambrecht, A., Fischer, A., and Kuhn, M.: Quantifying changes and trends in glacier area and volume in the Austrian Ötztal Alps (1969-1997-2006), The Cryosphere, 3, 205–215, doi: 10.5194/tc-3-205-2009, 2009.

Al-Mukhtar, M.: Random forest, support vector machine, and neural networks to modelling suspended sediment in Tigris River-Baghdad, Environ. Monit. Assess., 191, 673, doi: 10.1007/s10661-019-7821-5, 2019.

Laser- und Luftbildatlas Tirol: https://lba.tirol.gv.at/public/karte.xhtml, last access: 17 June 2022.

Antoniazza, G. and Lane, S. N.: Sediment yield over glacial cycles: A conceptual model, Prog. Phys. Geogr. Earth Environ., 842–865, doi: 10.1177/0309133321997292, 2021.

Beniston, M., Farinotti, D., Stoffel, M., Andreassen, L. M., Coppola, E., Eckert, N., Fantini, A., Giacona, F., Hauck, C., Huss, M., Huwald, H., Lehning, M., López-Moreno, J.-I., Magnusson, J., Marty, C., Morán-Tejéda, E., Morin, S., Naaim, M., Provenzale, A., Rabatel, A., Six, D., Stötter, J., Strasser, U., Terzago, S., and Vincent, C.: The European mountain cryosphere: a review of its current state, trends, and future challenges, The Cryosphere, 12, 759–794, doi: 10.5194/tc-12-759-2018, 2018.

Bergmann, H. and Reinwarth, O.: Die Pegelstation Vernagtbach (Ötztaler Alpen) - Planung, Bau und Messergebnisse, Z. Für Gletscherkunde Glazialgeol., 157–180, 1977.

Bilotta, G. S. and Brazier, R. E.: Understanding the influence of suspended solids on water quality and aquatic biota, Water Res., 42, 2849–2861, doi: 10.1016/j.watres.2008.03.018, 2008.

Braun, L. N., Escher-Vetter, H., Siebers, M., and Weber, M.: Water Balance of the highly Glaciated Vernagt Basin, Ötztal Alps, in: The water balance of the alps: what do we need to protect the water resources of the Alps? Proceedings of the conference held at Innsbruck university, 28 - 29 september 2006, Univ. Press, Innsbruck, 2007.

Breiman, L.: Random Forests, Mach. Learn., 45, 5–32, doi: 10.1023/A:1010933404324, 2001.

Breiman, L., Friedman, J. H., Olshen, R. A., and Stone, C. J.: Classification And Regression Trees, Routledge, New York, 368 pp., 1984.

Buckel, J. and Otto, J.-C.: The Austrian Glacier Inventory GI 4 (2015) in ArcGis (shapefile) format [data set], doi: 10.1594/PANGAEA.887415, 2018.

Carrivick, J. L. and Heckmann, T.: Short-term geomorphological evolution of proglacial systems, Geomorphology, 287, 3–28, doi: 10.1016/j.geomorph.2017.01.037, 2017.

Chiarle, M., Geertsema, M., Mortara, G., and Clague, J. J.: Relations between climate change and mass movement: Perspectives from the Canadian Cordillera and the European Alps, Glob. Planet. Change, 202, 103499, doi: 10.1016/j.gloplacha.2021.103499, 2021.

Costa, A., Molnar, P., Stutenbecker, L., Bakker, M., Silva, T. A., Schlunegger, F., Lane, S. N., Loizeau, J.-L., and Girardclos, S.: Temperature signal in suspended sediment export from an Alpine catchment, Hydrol. Earth Syst. Sci., 22, 509–528, doi: 10.5194/hess-22-509-2018, 2018.

Delaney, I. and Adhikari, S.: Increased Subglacial Sediment Discharge in a Warming Climate: Consideration of Ice Dynamics, Glacial Erosion, and Fluvial Sediment Transport, Geophys. Res. Lett., 47, e2019GL085672, doi: https://doi.org/10.1029/2019GL085672, 2020.

eHYD: Hydrographic Service, Austria, Bundesministerium für Landwirtschaft, Regionen und Tourismus, https://ehyd.gv.at/ [data set], 2021.

Escher-Vetter, H.: Climate change informationas derived from long-term measurements of winter and summer mass balance, in: Extended Abstracts, 29th International Conference on Alpine Meteorology, Chambéry, France, 465–468, 2007.

Escher-Vetter, H. and Siebers, M.: Sensitivity of glacier runoff to summer snowfall events, Ann. Glaciol., 46, 309–315, doi: 10.3189/172756407782871251, 2007.

Escher-Vetter, H., Oerter, H., Reinwarth, O., Braun, L. N., and Weber, M.: Hydrological and meteorological records from the Vernagtferner Basin - Vernagtbach station, for the years 1970 to 2001, [data set], doi: 10.1594/PANGAEA.775113, 2012.

Escher-Vetter, H., Braun, L. N., and Siebers, M.: Hydrological and meteorological records from the Vernagtferner Basin - Vernagtbach station, for the years 2002 to 2012 [data set], doi: 10.1594/PANGAEA.829530, 2014.

Francke, T., López-Tarazón, J. A., and Schröder, B.: Estimation of suspended sediment concentration and yield using linear models, random forests and quantile regression forests, Hydrol. Process., 22, 4892–4904, doi: 10.1002/hyp.7110, 2008a.

Francke, T., López-Tarazón, J. A., Vericat, D., Bronstert, A., and Batalla, R. J.: Flood-based analysis of high-magnitude sediment transport using a non-parametric method, Earth Surf. Process. Landf., 33, 2064–2077, doi: 10.1002/esp.1654, 2008b.

Gabbud, C. and Lane, S. N.: Ecosystem impacts of Alpine water intakes for hydropower: the challenge of sediment management, WIREs Water, 3, 41–61, doi: 10.1002/wat2.1124, 2016.

Guillén-Ludeña, S., Manso, P. A., and Schleiss, A. J.: Multidecadal Sediment Balance Modelling of a Cascade of Alpine Reservoirs and Perspectives Based on Climate Warming, Water, 10, 1759, doi: 10.3390/w10121759, 2018.

Hallet, B., Hunter, L., and Bogen, J.: Rates of erosion and sediment evacuation by glaciers: A review of field data and their implications, Glob. Planet. Change, 12, 213–235, doi: 10.1016/0921-8181(95)00021-6, 1996.

Hanus, S., Hrachowitz, M., Zekollari, H., Schoups, G., Vizcaino, M., and Kaitna, R.: Future changes in annual, seasonal and monthly runoff signatures in contrasting Alpine catchments in Austria, Hydrol. Earth Syst. Sci., 25, 3429–3453, doi: 10.5194/hess-25-3429-2021, 2021.

Hanzer, F., Förster, K., Nemec, J., and Strasser, U.: Projected cryospheric and hydrological impacts of 21st century climate change in the Ötztal Alps (Austria) simulated using a physically based approach, Hydrol. Earth Syst. Sci., 22, 1593–1614, doi: https://doi.org/10.5194/hess-22-1593-2018, 2018.

Herman, F., De Doncker, F., Delaney, I., Prasicek, G., and Koppes, M.: The impact of glaciers on mountain erosion, Nat. Rev. Earth Environ., 2, 422–435, doi: 10.1038/s43017-021-00165-9, 2021.

Hinderer, M., Kastowski, M., Kamelger, A., Bartolini, C., and Schlunegger, F.: River loads and modern denudation of the Alps — A review, Earth-Sci. Rev., 118, 11–44, doi: 10.1016/j.earscirev.2013.01.001, 2013.

Huggel, C., Salzmann, N., Allen, S., Caplan-Auerbach, J., Fischer, L., Haeberli, W., Larsen, C., Schneider, D., and Wessels, R.: Recent and future warm extreme events and high-mountain slope stability, Philos. Trans. R. Soc. Math. Phys. Eng. Sci., 368, 2435–2459, doi: 10.1098/rsta.2010.0078, 2010.

Huggel, C., Clague, J. J., and Korup, O.: Is climate change responsible for changing landslide activity in high mountains?, Earth Surf. Process. Landf., 37, 77–91, doi: 10.1002/esp.2223, 2012.

Huss, M., Bookhagen, B., Huggel, C., Jacobsen, D., Bradley, R. S., Clague, J. J., Vuille, M., Buytaert, W., Cayan, D. R., Greenwood, G., Mark, B. G., Milner, A. M., Weingartner, R., and Winder, M.: Toward mountains without permanent snow and ice, Earths Future, 5, 418–435, doi: 10.1002/2016EF000514, 2017.

Hydrographic yearbook of Austria: Hydrographisches Jahrbuch von Österreich, Hydrographischer Dienst in Österreich, Bundesministerium für Land- und Forstwirtschaft, Umwelt und Wasserwirtschaft Abteilung VII/3, 2016.

Institute of Meteorology and Geophysics: Climate Data Vent, Ötztal Alps, 1935-2011 [data set], doi: 10.1594/PANGAEA.806582, 2013.

Juen, I. and Kaser, G.: Climate Data Vent, Ötztal Alps, 2012-2016 [data set], doi: 10.1594/PANGAEA.876595, 2017.

Kormann, C., Bronstert, A., Francke, T., Recknagel, T., and Graeff, T.: Model-Based Attribution of High-Resolution Streamflow Trends in Two Alpine Basins of Western Austria, Hydrology, 3, 7, doi: 10.3390/hydrology3010007, 2016.

Kuhn, M., Nickus, U., and Pellet, F.: Precipitation Patterns in the Inner Ötztal, 17. Internationale Tagung für Alpine Meteorologie, Offenbach am Main, 1982.

Kuhn, M., Helfricht, K., Ortner, M., Landmann, J., and Gurgiser, W.: Liquid water storage in snow and ice in 86 Eastern Alpine basins and its changes from 1970–97 to 1998–2006, Ann. Glaciol., 57, 11–18, doi: 10.1017/aog.2016.24, 2016.

Lalk, P., Haimann, M., and Habersack, H.: Monitoring, Analyse und Interpretation des Schwebstofftransportes an österreichischen Flüssen, Österr. Wasser- Abfallwirtsch., 66, 306–315, doi: 10.1007/s00506-014-0175-x, 2014.

Land Tirol: Digital terrain model of Tyrol, 10m resolution, EPSG 31254 [data set], https://www.data.gv.at/katalog/dataset/land-tirol_tirolgelnde, 2016.

Land Tirol: tiris OGD map service “Wasser” [data set], https://www.data.gv.at/ katalog/dataset/0b5d6529-d88c-46c0-84f7-b37282e96ce8, 2021.

Lane, S. N., Bakker, M., Gabbud, C., Micheletti, N., and Saugy, J.-N.: Sediment export, transient landscape response and catchment-scale connectivity following rapid climate warming and Alpine glacier recession, Geomorphology, 277, 210–227, doi: 10.1016/j.geomorph.2016.02.015, 2017.

Lane, S. N., Bakker, M., Costa, A., Girardclos, S., Loizeau, J.-L., Molnar, P., Silva, T., Stutenbecker, L., and Schlunegger, F.: Making stratigraphy in the Anthropocene: climate change impacts and economic conditions controlling the supply of sediment to Lake Geneva, Sci. Rep., 9, 8904, doi: 10.1038/s41598-019-44914-9, 2019.

Leggat, M. S., Owens, P. N., Stott, T. A., Forrester, B. J., Déry, S. J., and Menounos, B.: Hydro-meteorological drivers and sources of suspended sediment flux in the pro-glacial zone of the retreating Castle Creek Glacier, Cariboo Mountains, British Columbia, Canada, Earth Surf. Process. Landf., 40, 1542–1559, doi: 10.1002/esp.3755, 2015.

Lindeløv, J. K.: mcp: An R Package for Regression With Multiple Change Points [code], OSF Preprints, doi: 10.31219/osf.io/fzqxv, 5 January 2020.

Madsen, H., Lawrence, D., Lang, M., Martinkova, M., and Kjeldsen, T. R.: Review of trend analysis and climate change projections of extreme precipitation and floods in Europe, J. Hydrol., 519, 3634–3650, doi: 10.1016/j.jhydrol.2014.11.003, 2014.

Mallakpour, I. and Villarini, G.: A simulation study to examine the sensitivity of the Pettitt test to detect abrupt changes in mean, Hydrol. Sci. J., 61, 245–254, doi: 10.1080/02626667.2015.1008482, 2016.

Mao, L., Comiti, F., Carrillo, R., and Penna, D.: Sediment Transport in Proglacial Rivers, Geomorphol. Proglacial Syst., 199–217, doi: 10.1007/978-3-319-94184-4_12, 2019.

Meinshausen, N.: Quantile Regression Forests, J. Mach. Learn. Res., 7, 983–999, 2006.

Merten, G., Capel, P., and Minella, J. P. G.: Effects of suspended sediment concentration and grain size on three optical turbidity sensors, J. Soils Sediments, 14, doi: 10.1007/s11368-013-0813-0, 2014.

Micheletti, N. and Lane, S. N.: Water yield and sediment export in small, partially glaciated Alpine watersheds in a warming climate, Water Resour. Res., 52, 4924–4943, doi: 10.1002/2016WR018774, 2016.

Moriasi, D. N., Arnold, J. G., Van Liew, M. W., Bingner, R. L., Harmel, R. D., and Veith, T. L.: Model Evaluation Guidelines for Systematic Quantification of Accuracy in Watershed Simulations, Trans. ASABE, 50, 885–900, doi: 10.13031/2013.23153, 2007.

Naeser, T.: Schwebstoffuntersuchungen am Gletscherbach des Vernagtferners in den Zentralen Ötztaler Alpen, Diploma thesis, Ludwig-Maximilians-Universität München, München, 92 pp., 2002.

Nones, M.: Dealing with sediment transport in flood risk management, Acta Geophys., 67, 677–685, doi: 10.1007/s11600-019-00273-7, 2019.

Pettitt, A. N.: A Non-Parametric Approach to the Change-Point Problem, J. R. Stat. Soc. Ser. C Appl. Stat., 28, 126–135, doi: 10.2307/2346729, 1979.

Pilz, T., Delgado, J. M., Voss, S., Vormoor, K., Francke, T., Costa, A. C., Martins, E., and Bronstert, A.: Seasonal drought prediction for semiarid northeast Brazil: what is the added value of a process-based hydrological model?, Hydrol. Earth Syst. Sci., 23, 1951–1971, doi: 10.5194/hess-23-1951-2019, 2019.

Pohlert, T.: trend: Non-Parametric Trend Tests and Change-Point Detection. R package version 1.1.2. [code], R, 2020.

R Core Team: R: A language and environment for statistical computing [code], R Foundation for Statistical Computing, Vienna, Austria, https://www.R-project.org/, 2018.

Rottler, E., Francke, T., Bürger, G., and Bronstert, A.: Long-term changes in central European river discharge for 1869–2016: impact of changing snow covers, reservoir constructions and an intensified hydrological cycle, Hydrol. Earth Syst. Sci., 24, 1721–1740, doi: 10.5194/hess-24-1721-2020, 2020.

Rottler, E., Vormoor, K., Francke, T., Warscher, M., Strasser, U., and Bronstert, A.: Elevation-dependent compensation effects in snowmelt in the Rhine River Basin upstream gauge Basel, Hydrol. Res., 52, 536–557, doi: 10.2166/nh.2021.092, 2021.

Santander Meteorology Group: fume: FUME package. R package version 1.0. [code], R, Santander Meteorology Group, 2012.

Savi, S., Comiti, F., and Strecker, M. R.: Pronounced increase in slope instability linked to global warming: A case study from the eastern European Alps, Earth Surf. Process. Landf., 46, doi: https://doi.org/10.1002/esp.5100, 2020.

Schaefli, B. and Gupta, H. V.: Do Nash values have value?, Hydrol. Process., 21, 2075–2080, doi: 10.1002/hyp.6825, 2007.

Schmidt, L. K. and Hydrographic Service of Tyrol, Austria: Discharge and suspended sediment time series of 2006–2020 of gauges Vent Rofenache and Tumpen in the glacierized high alpine Ötztal, Tyrol, Austria [data set], DOI: 10.23728/b2share.be13f43ce9bb46d8a7eedb7b56df3140, 2021.

Schmidt, L. K., Grosse, P. M., and Francke, T.: A Quantile Regression Forests approach for sedigraph-reconstruction and sediment yield calculation [data set], DOI: 10.23728/b2share.109960a9fb42427b9d0a85b998b9d18c, 2022a.

Schmidt, L. K., Francke, T., Rottler, E., Blume, T., Schöber, J., and Bronstert, A.: Suspended sediment and discharge dynamics in a glaciated alpine environment: identifying crucial areas and time periods on several spatial and temporal scales in the Ötztal, Austria, Earth Surf. Dyn., 10, 653–669, doi: https://doi.org/10.5194/esurf-10-653-2022, 2022b.

Schmieder, J., Garvelmann, J., Marke, T., and Strasser, U.: Spatio-temporal tracer variability in the glacier melt end-member — How does it affect hydrograph separation results?, Hydrol. Process., 32, 1828–1843, doi: 10.1002/hyp.11628, 2018.

Schöber, J. and Hofer, B.: The sediment budget of the glacial streams in the catchment area of the Gepatsch reservoir in the Ötztal Alps in the period 1965-2015, in: ICOLD (International Comission on Large Dam Systems) Proceedings, Twenty-Sixth International Congress on Large Dams, Vienna, Austria, 2018.

Schöber, J., Schneider, K., Helfricht, K., Schattan, P., Achleitner, S., Schöberl, F., and Kirnbauer, R.: Snow cover characteristics in a glacierized catchment in the Tyrolean Alps - Improved spatially distributed modelling by usage of Lidar data, J. Hydrol., 519, 3492–3510, doi: 10.1016/j.jhydrol.2013.12.054, 2014.

Sen, P. K.: Estimates of the Regression Coefficient Based on Kendall's Tau, J. Am. Stat. Assoc., 63, 1379–1389, doi: 10.1080/01621459.1968.10480934, 1968.

Sommer, C., Malz, P., Seehaus, T. C., Lippl, S., Zemp, M., and Braun, M. H.: Rapid glacier retreat and downwasting throughout the European Alps in the early 21 st century, Nat. Commun., 11, 3209, doi: 10.1038/s41467-020-16818-0, 2020.

Strasser, U., Marke, T., Braun, L., Escher-Vetter, H., Juen, I., Kuhn, M., Maussion, F., Mayer, C., Nicholson, L., Niedertscheider, K., Sailer, R., Stötter, J., Weber, M., and Kaser, G.: The Rofental: a high Alpine research basin (1890–3770 m a.s.l.) in the Ötztal Alps (Austria) with over 150 years of hydrometeorological and glaciological observations, Earth Syst. Sci. Data, 10, 151–171, doi: https://doi.org/10.5194/essd-10-151-2018, 2018.

van Tiel, M., Kohn, I., Loon, A. F. V., and Stahl, K.: The compensating effect of glaciers: Characterizing the relation between interannual streamflow variability and glacier cover, Hydrol. Process., 34, doi: 10.1002/hyp.13603, 2019.

Tschada, H. and Hofer, B.: Total solids load from the catchment area of the Kaunertal hydroelectric power station: the results of 25 years of operation, in: Hydrology of Mountainous Regions--II: Artificial Reservoirs, Water and Slopes (Proceedings of two Lausanne Symposia), IAHS Publication, Lausanne, Switzerland, 8, 1990.

Turowski, J. M., Rickenmann, D., and Dadson, S. J.: The partitioning of the total sediment load of a river into suspended load and bedload: a review of empirical data, Sedimentology, 57, 1126–1146, doi: 10.1111/j.1365-3091.2009.01140.x, 2010.

Vercruysse, K., Grabowski, R. C., and Rickson, R. J.: Suspended sediment transport dynamics in rivers: Multi-scale drivers of temporal variation, Earth-Sci. Rev., 166, 38–52, doi: 10.1016/j.earscirev.2016.12.016, 2017.

Vormoor, K., Lawrence, D., Heistermann, M., and Bronstert, A.: Climate change impacts on the seasonality and generation processes of floods - projections and uncertainties for catchments with mixed snowmelt/rainfall regimes, Hydrol. Earth Syst. Sci., 19, 913–931, doi: 10.5194/hess-19-913-2015, 2015.

Weber, M. and Prasch, M.: Influence of the Glaciers on Runoff Regime and Its Change, in: Regional Assessment of Global Change Impacts, edited by: Mauser, W. and Prasch, M., Springer International Publishing, Cham, 493–509, doi: 10.1007/978-3-319-16751-0_56, 2016.

Wijngaard, R. R., Helfricht, K., Schneeberger, K., Huttenlau, M., Schneider, K., and Bierkens, M. F. P.: Hydrological response of the Ötztal glacierized catchments to climate change, Hydrol. Res., 47, 979–995, doi: 10.2166/nh.2015.093, 2016.

World Glacier Monitoring Service: Fluctuations of Glaciers Database, WGMS [data set], doi: 10.5904/wgms-fog-2021-05, 2021.

Yue, S. and Wang, C.: The Mann-Kendall Test Modified by Effective Sample Size to Detect Trend in Serially Correlated Hydrological Series, Water Resour. Manag., 18, 201–218, doi: 10.1023/B:WARM.0000043140.61082.60, 2004.

Yue, S., Kundzewicz, Z. W., and Wang, L.: Detection of Changes, in: Changes in Flood Risk in Europe, edited by: Kundzewicz, Z. W., IAHS Press, Wallingford, 387–408, 2012.

Zimmermann, A., Francke, T., and Elsenbeer, H.: Forests and erosion: Insights from a study of suspended-sediment dynamics in an overland flow-prone rainforest catchment, J. Hydrol., 428–429, 170–181, doi: 10.1016/j.jhydrol.2012.01.039, 2012.

https://doi.org/10.5194/egusphere-2022-616
Preprint. Discussion started: 29 August 2022

Appendix A

Table A1: Characteristics of input data. Q = discharge, T = temperature, P = precipitation, SSC = suspended sediment concentration. HD = Hydrographic Service of the State of Tyrol, Austria. BAdW = Bavarian Academy of Sciences and Humanities, Munich, Germany.

Variable	Location	Coordinates (lon, lat; WGS84)	Length	Temporal resolution	Source	Availability
Q	Vent	10 54 39, 46 51 25	01.01.1967 – 31.12.2017	Daily means	HD	(eHYD, 2021)
			01.01.1967 – 31.12.2020	15-minute mean		Can be requested via wasserwirtschaft@tirol.gv.at
T, P	Vent	10 54 46, 46 51 26	01.01.1935 – 31.12.2011	Daily mean (T) and sum (P)	Institute of Meteorology and Geophysics, Innsbruck, Austria	(Institute of Meteorology and Geophysics, 2013)
			01.01.2012 – 31.12.2016	Daily mean (T) and sum (P)	Institute of Atmospheric and Cryospheric Sciences, Innsbruck, Austria	(Juen and Kaser, 2017)
			01.01.2017 – 31.12.2020	Daily mean (T) and sum (P)	HD	Can be requested via wasserwirtschaft@tirol.gv.at
SSC (turbidity)	Vent	10 54 39, 46 51 25	01.05.2006 – 31.10.2020	15-minute mean	HD	(Schmidt and Hydrographic Service of Tyrol, Austria, 2021)
Q, P, T	Vernagt	10 49 43, 46 51 24	01.05.1974 – 31.10.2001	60-minute mean	BAdW	(Escher-Vetter et al., 2012)
Q	Vernagt		01.05.2000 – 20.10.2001	10-minute mean		
Q, P, T	Vernagt		01.05.2002 – 31.12.2012	5-minute mean		(Escher-Vetter et al., 2014)
Q, P, T	Vernagt		01.05.2013 – 15.10.2020	5-minute mean		Data will successively be made available on PANGEA.
SSC (turbidity)	Vernagt		01.05.2000 – 20.10.2001	10-minute mean		
SSC (turbidity)	Vernagt		30.04.2019 – 03.11.2020	5-minute mean		
SSC samples	Vernagt		23.05.2019 – 30.08.2020	131 samples	This study	
T, P	Vernagt (HD)	10 49 42, 46 51 24	07.10.2010 – 31.12.2020	15 minute mean (T) and sum (P)	HD	Can be requested via wasserwirtschaft@tirol.gv.at
T, P	Martin-Busch-Hütte	10 53 18 46 48 03	23.09.2010 – 31.12.2020	15-minute mean (T) and sum (P)	HD	Can be requested via wasserwirtschaft@tirol.gv.at

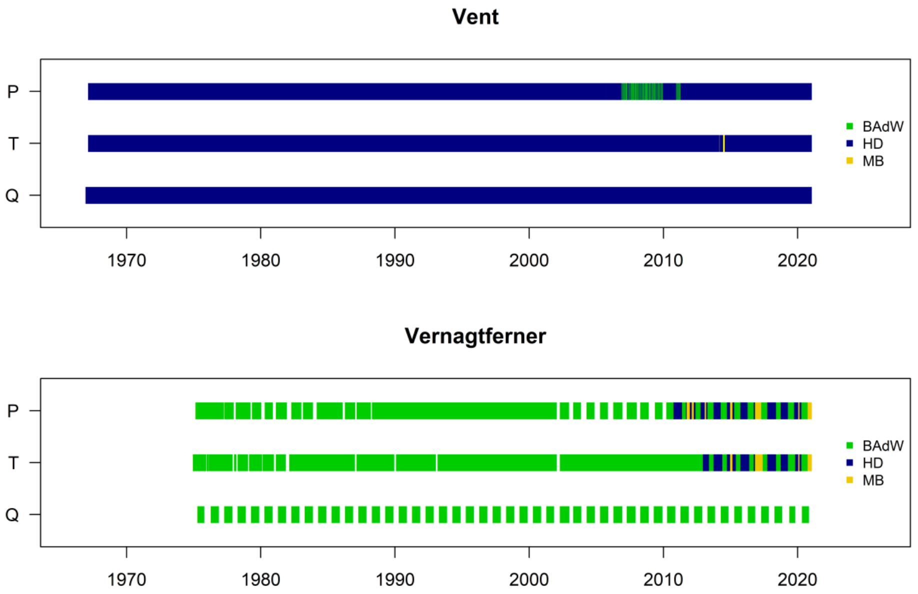

Figure A1 Discharge (Q), Temperature (T) and Precipitation (P) data at the two gauges after gap-filling procedure. The color indicates the data source (BAdW = Bavarian Academy of Sciences and Humanities, HD = Hydrographic Service of Tyrol stations at gauges Vent (top) and Vernagt (bottom), MB = Martin-Busch Hütte).